## Subproject E2.3

# Behavior of Cells in 2D and 3D Micro- and Nanostructured Patterns


## Principle Investigator: Martin Bastmeyer

**CFN-Financed Scientists: Zhongxiang Jiang (2005-2009), Franziska Klein (2005-2010), Tatjana Autenrieth (2011), Benjamin Richter (2011)**

**Further Scientists: Dr. Anne von Philipsborn (2005-2007), Dr. Zhongxiang Jiang (2009-2010), Alexandra Greiner (since 2010), Guillaume Delaittre (since 2010), Tatjana Autenrieth (2008-2010)**

**Zoologisches Institut**
**Zell- und Neurobiologie**
**KIT**

**E2.3** Bastmeyer

## Behavior of Cells in 2D and 3D Micro- and Nanostructured Patterns

### Introduction and Summary

Studying cell behavior in response to the presentation of selected chemical or physical stimuli in a cell culture environment is a well established and successful strategy in cell biology. Due to current limitations in our experimental models, we still lack a comprehensive understanding of how different extracellular cues in the natural environment of tissues or organisms are integrated to control cell behavior. During the last years, the importance of physical properties, such as mechanical stiffness, topography of the cellular environment, or the spatial patterns of ligand presentation is recognized to have a profound influence on cell behavior and differentiation. The geometry of ligand presentation spans different length scales, ranging from nanoscale distributions at the cell membrane to several micrometers for the arrangement of single sites of adhesion at the cellular level. In addition, graded distributions of ligands and signaling molecules play major roles during development and regeneration of multicellular organisms. Studies on the influence of spatial 2D ligand distributions have been made possible by the introduction of microcontact printing (μCP) of extracellular matrix (ECM) molecules or related techniques. These studies have shown that the spatial distribution of ligands has a crucial impact on several key physiological aspects including cell survival and cell proliferation. In addition to the geometry of ligand presentation, the stiffness of the environment has emerged as an additional regulator of cell behavior and fate. It has been shown that cell organization and differentiation changes dramatically as cells are plated on increasingly softer 2D substrates.

However, cells grown on 2D tissue culture substrates often differ considerably in morphology, cell-cell and cell-matrix interactions, and differentiation from those growing in more physiological 3D environments. *In vitro* 3D models currently used include scaffolds generated from purified ECM molecules and synthetic biomaterials. Nonetheless, the geometry and physical properties of these 3D scaffolds are often hard to control

In this subproject we are using different methods to reliably pattern 2D growth substrates with biomolecules at the micro- and nanometer level. In addition, we are developing methods to produce arbitrary 3D structures for the study of cell growth.

## 1. Two-dimensional patterned substrates

### 1.1 Theoretical modeling of cell shape on micropatterned substrates:

Using microcontact printing (Lehnert et al., 2004), we further studied the geometrical limits of cell adhesion. In cooperation with Ulrich Schwarz (formerly E2.5, now University Heidelberg) we developed a theoretical model to describe the cell shape on these micropatterned substrates (Bischofs et al., 2008). In this study, we identify common shape determinants spanning cell and tissue scales. For cells whose sites of adhesion are restricted to small adhesive islands on a micropatterned substrate, the shape resembles a sequence of inward-curved circular arcs (Fig. 1).

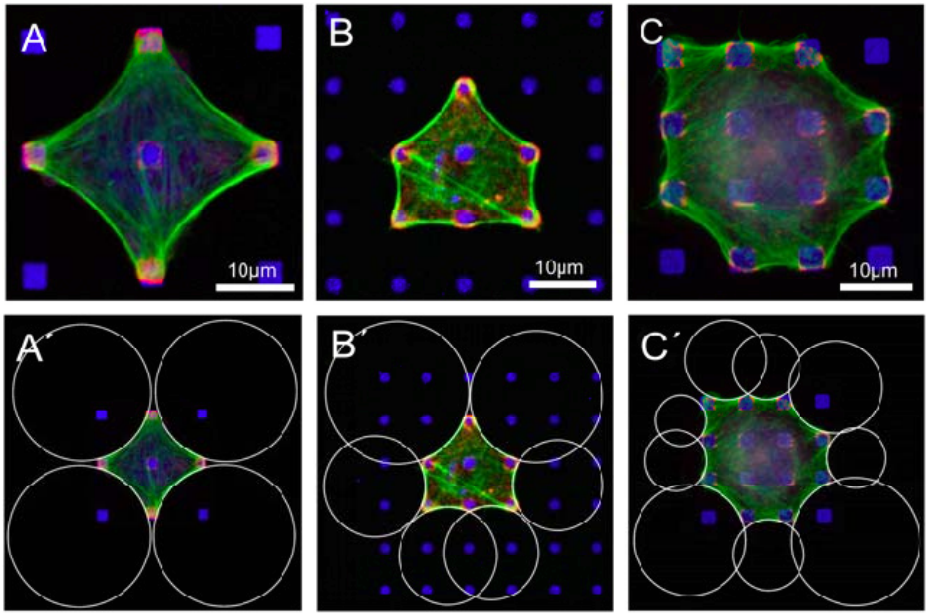


**Figure 1** Cell shape on micropatterned substrates. **(A–C)** Arc-like contours composed of actin fibers characterize the shape of BRL (A and B) and B16 cells **(C)** cultured on substrates of micropatterned fibronectin dots. Cultures were labeled for actin (green), paxillin (red), and fibronectin (blue). Scale bars: 10 µm. (A9–C9) For all cases, arc-like contours fit well to circles determined by custom-made software. **(B and C)** The circles spanning diagonal distances show larger radii than the circles spanning the shorter distances between neighboring adhesions.

Earlier studies have interpreted the arc-like shape features as indicating the validity of the Laplace law, which describes the shape of inanimate matter under tension (for example, soap bubbles). However, we find experimentally that, radii increase with spanning distance between adhesion points (Fig. 2). Such a relation cannot be explained from the local considerations resulting in the Laplace law and implies that the distribution of tension in cellular systems is more complex, including a dependence on boundary conditions. Yet and despite the underlying molecular complexity, the relation leads to surprisingly universal shapes both on cell and tissue levels. To explain our experimental findings, we use theoretical modeling and computer simulations to identify filamentous network mechanics and active contractility to be the unifying principles bridging cell and tissue scales.

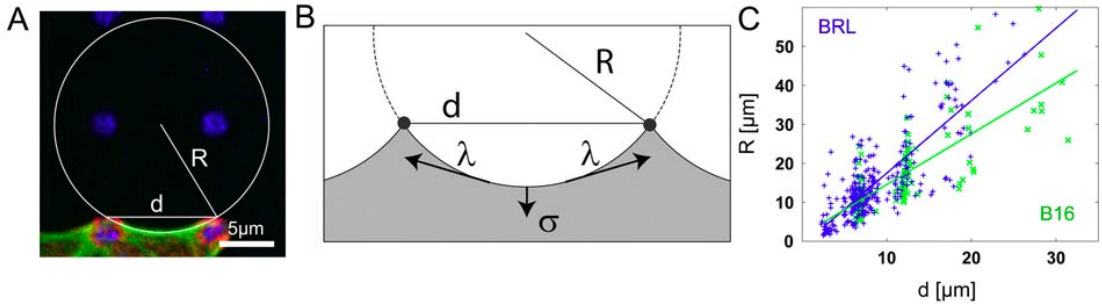


**Figure 2** R-d relation. **(A)** For each arc, radius R and spanning distance d are recorded. **(B)** Simple tension model: Line tension l straightens the contour between neighboring adhesions, whereas surface tensions pulls the envelope inward towards the bulk. In mechanical equilibrium, the local radius of curvature is R ¼ l/s and does not depend on the spanning distance d. **(C)** For both, BRL (blue) and B16 (green) cells, arc radius R increases with spanning distance d.

In particular, we derive a modified Laplace law that can explain our experimental findings in a quantitative manner. This novel type of Laplace law is first confirmed by computer simulations and then derived as a self-consistent equation for arc radius as a function of spanning distance. We show that our model implies two different control modes (tension versus elasticity control) that, for cells, correspond to two essential parts of Rho signaling to the cytoskeleton, namely reorganization of the actin cytoskeleton and activation of myosin II motors.

Cells that spread in a well defined 3D scaffold (see below) develop similar arc-like shape features. At present we are investigating, in collaboration with the group of Ulrich Schwarz, whether the same rules and theoretical models apply for cell forms in 3D.

### 1.2 Quantification of cell size in relation to fibronectin coverage

In this project we systematically study the influence of both geometry and ECM density on cell signaling and cell spreading for three different cell types (B16 fibroblast-like mouse melanoma skin cell line, BRL parenchymal rat liver cells, and A549 lung epithelial cell line) by using µCP. Different substrate geometries were combined with coatings of variable dilutions of fibronectin (FN). To remain the total protein amount constant, active FN was mixed with biologically inactive, heat-inactivated FN (Fig. 3).

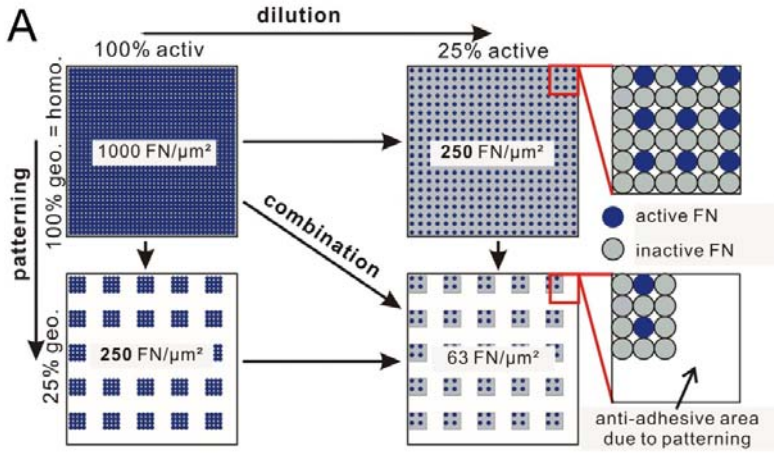


**Figure 3** Cell size in relation to fibronectin (FN) coverage. Patterned substrates produced with microcontact printing (µCP) were combined with coatings of variable dilutions of biologically-active FN diluted with heat-inactivated FN. This enables the preparation of different substrate geometries with variable densities of FN binding sites.

The area covered by the three cell types was measured on different patterns with a variable FN surface coverage, on uncoated substrata (0% FN coverage) and on homogeneous FN substrata (100% coverage). A 100% coverage roughly corresponds to 1000 FN molecules per µm². On these homogeneous substrates B16 fibroblast-like cells spread over an area of 1100 µm² (Fig. 4C), whereas epithelial A549 cells reach a mean size of about 1800µm$^2$ (Fig. 4A). BRL cells of parenchymal origin show an intermediate behavior and spread over an area of about 1500 µm² (Fig. 4B). Despite differences in maximum cell size, a quantitative analysis of cell spreading on patterned substrates revealed remarkable similarities between the different cell types. Irrespective of substrate geometry or FN dilution, a positive correlation between cell size and effective FN-coverage was observed (Fig. 4).

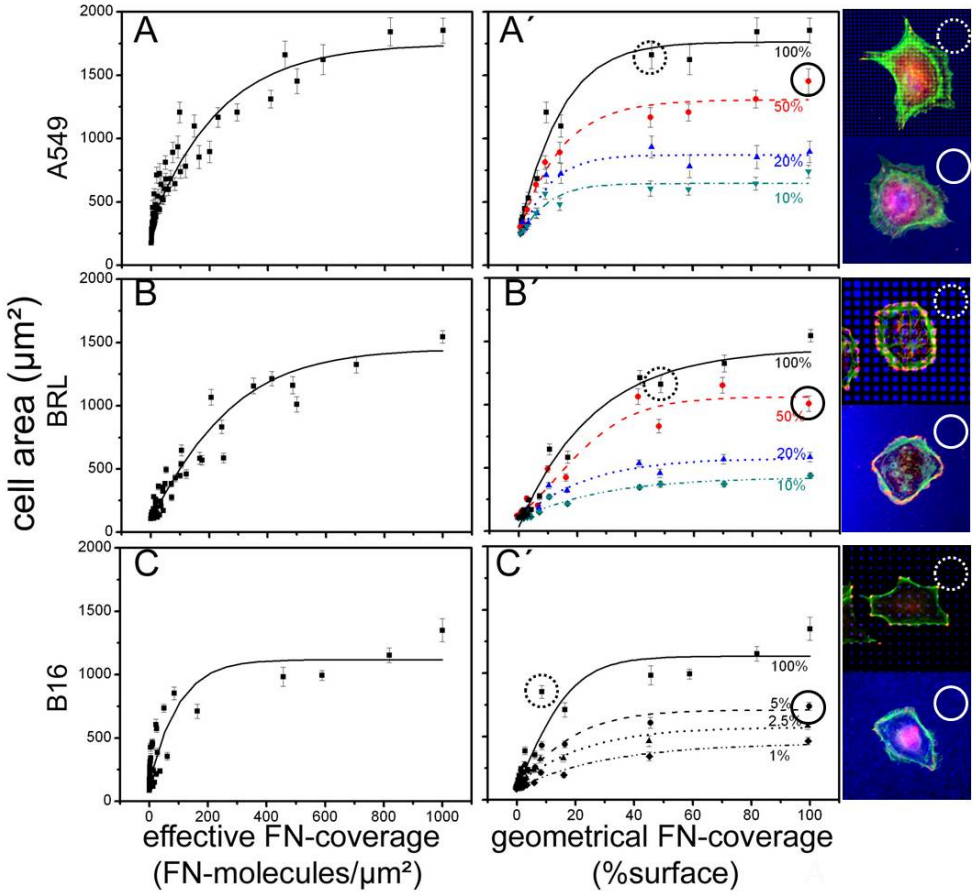


**Figure 4** Cell sizes of three different cell types plotted against the effective and geometrical fibronectin (FN) coverage. The percentage of biologically-active FN is shown in different colors. Plotting cell size against the absolute number of active FN molecules indicates that cell size is positively correlated with the effective FN coverage irrespective of substrate geometry, FN dilution, or cell type.

In addition, the cell lines differ considerately in their requirements on available FN ligands. B16 cells reach an optimal spreading size already at a surface coating above 15% and a half maximum spreading is induced by 5% coverage with FN (Fig. 4C). In contrast, half maximum spreading for A549 cells is already observed at 50% coverage (Fig. 4A), whereas BRL cell show an intermediate

behavior (Fig. 4B). These findings indicate, that fibroblasts that *in vivo* grow in a sparse meshwork of ECM molecules within the connective tissue can tolerate lower FN concentrations than epithelia cells that usually grow *in vivo* on a ECM-dense basal lamina.

When cells interact with their growth substrate, integrin receptors bind to ECM molecules, cluster, and recruit a variety of intracellular signaling proteins like Paxillin or FAK. This recruitment plays a fundamental role in regulating cell spreading and migration. To examine the underlying mechanisms how cells read out their ECM environment, cells growing on patterned substrates with a variable FN surface coverage were immunolabeled against various cell-matrix contact markers such as Paxillin, pPaxillin, FAK, pFAK, or ß1-integrin and analyzed with a confocal microscope (Fig. 5). The contact markers show different distributions: integrins are concentrated on every FN-spot covered by the cells, whereas FAK and in particular pFAK are mainly found at contacts in the cell periphery. These findings are further supported by time-lapse studies with cell expressing GFP-tagged integrins or GFP-tagged Paxillin (not shown). Accordingly, a quantitative analysis reveals that only the area covered by ß1-integrin correlates with cell size (Fig. 5).

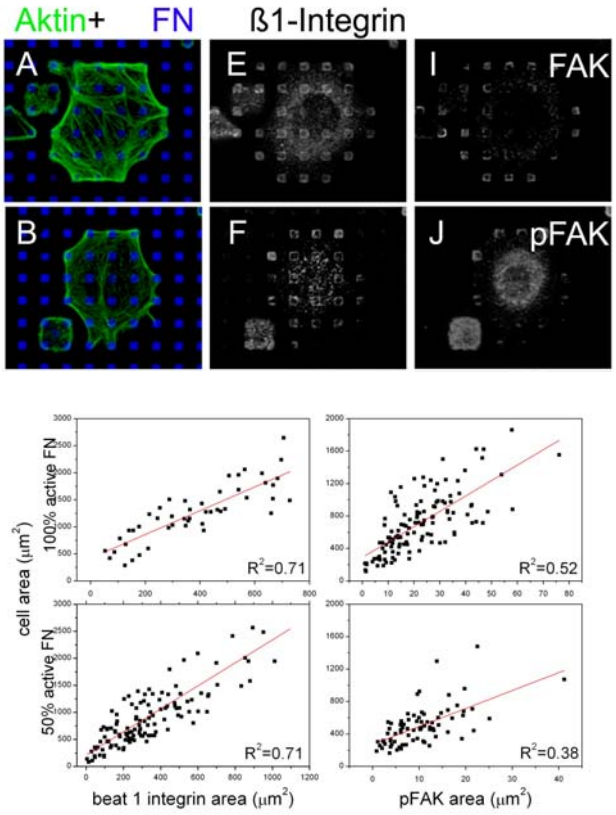


**Figure 5** A549 cells on micropatterned substrates labeled for actin, fibronectin (FN) and contact marker proteins (ß1-integrin, FAK, pFAK. The contact markers show different distributions: integrins are concentrated on every FN-spot covered by the cells, whereas FAK and in particular pFAK are mainly found at contacts in the cell periphery. Accordingly, only the area covered by ß1-Integrin correlates with cell size.

These findings suggest that cells cultured on micropatterned surfaces possess two different types of cell-substrate contact sites: Contacts in the cellular periphery (most probably those under tension) contain the whole set of classical focal adhesion contact markers, whereas contacts in the center of the cells mainly assemble integrin receptors and are used to measure the amount of ECM proteins (here FN) available for cell adhesion. A short communication on these findings has been published. A full manuscript is in preparation.

### 1.3 Substrate-bound gradients of biomolecules

Graded distributions of soluble and membrane-bound signaling molecules play fundamental roles during the development of multicellular organisms (von Philipsborn and Bastmeyer, 2007). During development of the nervous system, the correct navigation of axons to their target region is based on specific interactions with guidance factors, many of which are distributed in a graded way (Dickson, 2002). We used μCP to produce for the first time substrate-bound gradients of the axon guidance molecule ephrin (von Philipsborn et al., 2006a). The fabricated patterns consist of dots and lines, which are printed with a fixed printing ink concentration, but vary with respect to their size and spacing. In contrast to continuous gradients with smooth transitions between different concentrations, these gradients are discontinuous on a submicron scale (Fig. 6). We demonstrate that chick retinal axons are able to integrate these discontinuous ephrin distributions and stop at a distinct zone in the gradient. Quantitative analysis of axon outgrowth shows that the stop reaction is controlled by a combination of the local ephrin concentration and the total amount of encountered ephrin (von Philipsborn et al., 2006b).

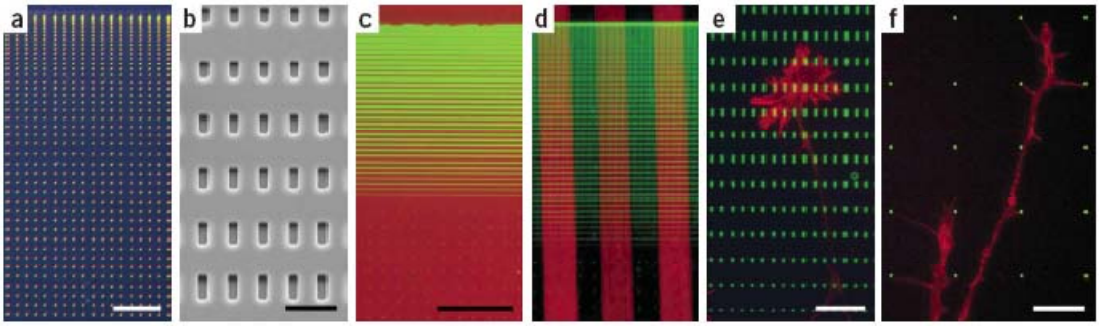


**Figure 6** Silicon masters and fluorescent protein patterns. **(a)** A silicon master with a graded pattern built up by dots imaged with the light microscope. **(b)** Dots etched into a silicon master (approximately 650 nm depth) seen with the scanning electron microscope. **(c,d)** Graded protein patterns visualized with the fluorescence microscope. The printed protein (ephrinA5) is shown in green, laminin covering the pattern is shown in red. In d, laminin was applied in stripes. **(e,f)** Growth cones navigating in protein patterns. The protein (ephrinA5) is shown in green, phalloidin-stained axonal actin in red. Scale bars: a,c,d, 100 μm; b, 5 μm; e,f, 15 μm.

Similar results were obtained with a different type of a graded ephrin distribution produced with microfluidic networks (von Philipsborn et al., 2007; Lang et al., 2008). Here, a substrate-bound stepwise protein gradient was fabricated by means of a microfluidic network etched into a silicon wafer with an array of parallel 14-micrometer– wide channels, which can be filled with a series of arbitrarily chosen protein solutions. In a subsequent μCP step, the protein pattern is transferred onto a surface and is used as a substrate for cell culture studies (Figure 7).

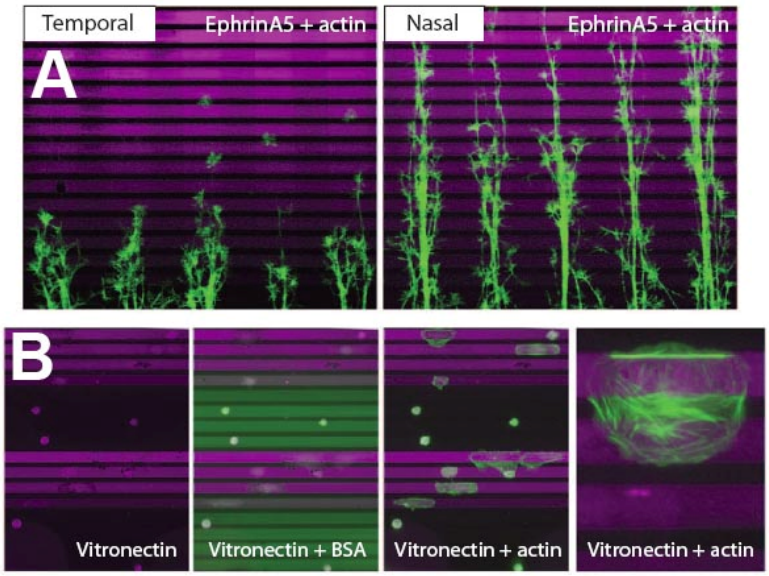


**Figure 7** Stepwise protein gradients produced with microfluidic networks. (**A**) Chick RGC axons (stained for actin, in green) growing on ephrinA5 gradients (purple) with overlaid laminin stripes. Temporal axons stop in the gradient, nasal axons advance up to the end of the gradient. (**B**) Patterns of two adjacent gradients built by lanes covered with vitronectin (purple) and BSA (green). BRL cells (stained for actin, in green) preferentially spread on the lanes with high vitronectin concentrations. Width of all shown µFN lanes is 14 µm.

In a further set of experiments we study polarization and directional migration of cells in an adhesive gradient (haptotaxis). Directional cell migration induced *in vitro* either by gradients of soluble signaling molecules (chemotaxis) or in the scratch assay is a well-studied phenomenon. It is widely accepted that during this cellular response the Par6/PKC complex plays a crucial role in establishing cell polarization. In contrast, much less is known about cell polarization and migration in substrate-bound adhesive protein gradients (haptotaxis).

We investigate cell polarization and migration of primary chicken fibroblasts in discontinuous adhesive FN-gradients. The gradients were prepared by µCP and consist of FN dots of 1 µm diameter. Their center-to-center spacing is kept constant along the x-axis but decreases along the y-axis, forming a linear gradient.

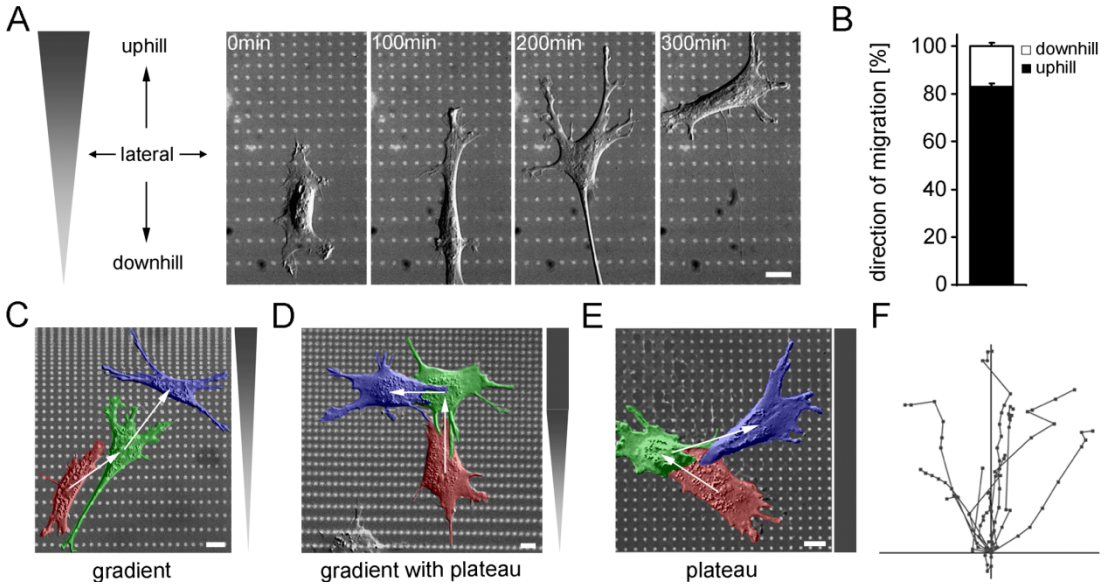


**Figure 8** Cell migration (haptotaxis) in adhesive gradients.

In these FN-gradients 80% of the cells migrate uphill (haptotaxis), 20% migrate downhill, but none were observed migrating perpendicular to the gradient. To investigate the role of cytoskeletal elements during haptotaxis, specific inhibitors were applied. Impairing myosin II function by treatment with either Y-27632 or blebbistatin results in cells that migrate randomly in any direction. This demonstrates that haptotaxis depends on the cellular ability to balance intracellular forces (Fig. 9A). In contrast, interfering with microtubule dynamics by treatment with either nocodazole or taxol leads to a random uphill or downhill migration. However, no cells were observed migrating perpendicular to the gradient (Fig. 9B). This indicates that cells with altered microtubule dynamics still recognize the FN gradient *per se* but are unable to distinguish between higher and lower FN coverage. The Par6/PKC complex links microtubules to the plasma membrane and mediates actin rearrangements and therefore might also be important for haptotaxis. Fibroblasts expressing a dominant-negative construct migrate randomly in our haptotaxis assays, indicating a function of the Par6/PKC complex.

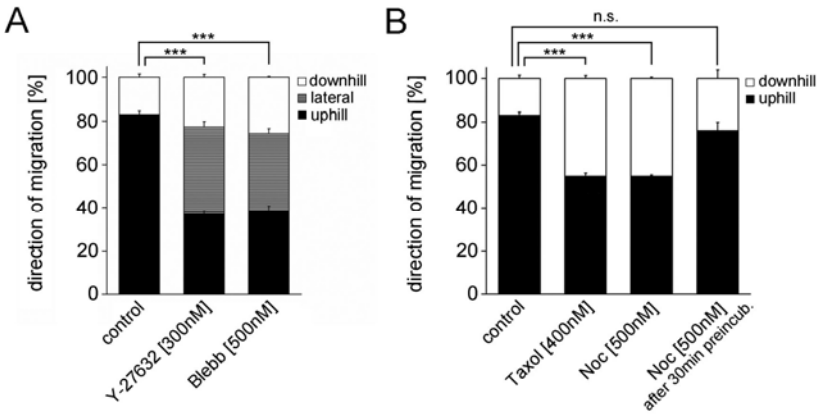


**Figure 9** Cell migration (haptotaxis) in adhesive fibronectin gradients after treatment with actin inhibitors (A) or microtubule inhibitors (B). Whereas actin inhibitors cause a random migration, microtubule inhibitors lead to a random uphill or downhill migration. Inhibition of microtubules 30 min after cell seeding has no effect on the direction of migration, indicating that the sensing of the gradient is an early event during haptotaxis.

In summary, primary chicken fibroblasts reveal a directed uphill migration in discontinuous adhesive FN-gradients. During haptotaxis a balance of intracellular forces and microtubule dynamics are necessary for gradient sensing. A short communication on these findings has been published (Autenrieth and Bastmeyer, 2010). A full manuscript is in preparation.

## 2. Three-dimensional patterned cell culture substrates

During recent years it has become clear that cells are not only influenced by biochemical cues but also by physical aspects like stiffness and geometry of the extracellular environment (Ross et al., 2011). These additional factors are simultaneously sensed on different length scales, ranging from nanoscale assembly processes at single sites of adhesion to microscale organization of the cytoskeleton. They have a major impact on cell fate and function, with dramatic consequences for tissue integrity. Recently, it has been demonstrated that also stem cell differentiation is influenced by the nano-topography and the stiffness of the growth substrate. Most of our current knowledge on cell behavior and differentiation is derived primarily from studies on rigid and planar two-dimensional (2D) tissue culture substrates. Therefore, there is an increasing demand for *in vitro* models that capture more of the relevant complexity present in three-dimensional (3D) tissue scaffolds. Technologies for fabricating macroscopic tissue architectures in the mm and µm range have become available during recent years (Greiner et al., 2011); however, methods to reliably design 3D cellular environments within the micrometer to nanometer range are still missing. Ideally, these substrates should have a controllable distribution of cell-substrate contact sites in the nanometer range and adjustable physical properties (for example, stiffness).

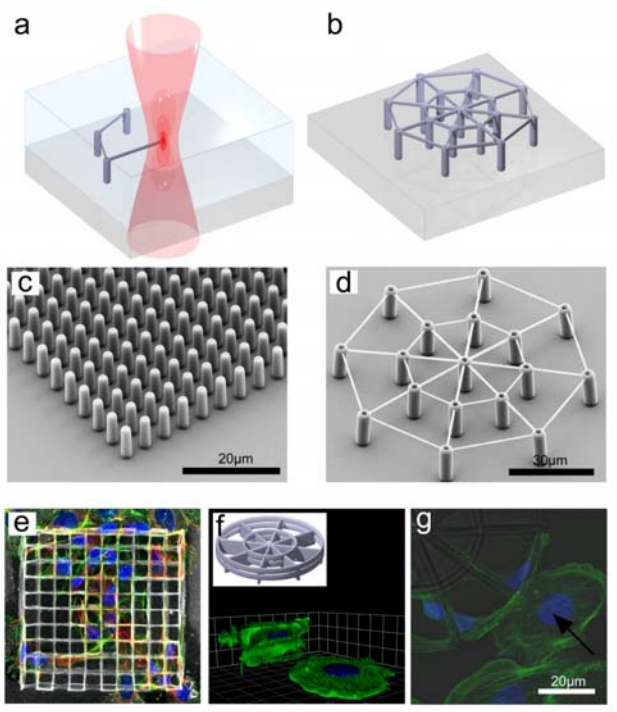


**Figure 8** Schematic drawing illustrating the Direct laser Writing (DLW) process to produce arbitrary 3D templates for cell growth studies (**a, b**). Scanning electron micrographs depicting templates with elevated topology yet 2.5-dimensional periodicity ("2.5D") (**c**) and true 3D templates (**d**). Top view of a woodpile structure populated with B16 cells (**e**). 3D-reconstruction (**f**) and top view (**g**) of two BRL cells demonstrating the difference in cell morphology when grown 3D vs. 2D. The insert in **f** shows a schematic drawing of the wheel-structure used for cell culture. Nuclei are labeled in blue and actin filaments in green in **e-f**.

In cooperation with the group of M. Wegener (A1.4) we are using Direct Laser Writing (DLW) by multiphoton-polymerization to produce tailored 3D environments for cell growth studies. DLW is a highly flexible technique for the fabrication of 3D objects with lateral dimensions in x, y and z coordinates of 300 µm and lattice constants varying between a few nanometer and several micrometers (Fig. 8a-d). In three physics Diploma theses, supervised and supported by CFN A1 scientists, a very large variety of different topologies and resist materials have been explored. This

work was accompanied by two PhD students from the biology department performing cell culture assays and microscopic analysis.

In the beginning, structures were produced using SU-8 as a photo resist and directly employed for cell culture. SU-8 structures, however, turned out to be inadequate because they hardly endure cell culture conditions and in addition show strong autofluorescence, which is perturbing for the subsequent confocal imaging step. Therefore, the SU-8 templates were coated with a thin silica film followed by subsequent removal of the SU-8 via calcination. This resulted in mechanically stable 3D glass templates with excellent optical properties for microscopic analysis. To determine the minimal feature sizes that can be invaded by growing cells, geometrically simple woodpile structures were initially employed. They resemble letter cases with a height of 30 µm and varying lattice constants of 2, 5, and 10 µm (Fig. 8e). These structures were homogeneously coated with ECM molecules and used as growth substrates for different cell types. These experiments revealed, that cells were able to completely invade 10 µm-woodpile structures (Fig. 8e), but only send out cell processes into 2 and 5 µm lattices.

Based on these findings, more complicated geometries were used for further investigations. The so called “Karlsruhe wheel” consists of two concentric rings connected by 8 spokes and offers a wide variety of different angles and distances in a single 3D structure (Fig. 8 f, insert). Cells cultured in these wheels adopt a true 3D growth pattern that considerably differs from the cell morphology on stiff 2D surfaces (Fig. 8 f,g). Long-term culture revealed that the substrates are biocompatible and that the amount of cell proliferation in 3D does not differ from proliferation in 2D. An extensive immunocytochemical investigation revealed that the composition of cell-substrate contact sites, e.g., Vinculin, FAK, Paxillin does not considerably differ from that observed in 2D cultures. Also the morphological distribution of intracellular structures like microtubules or the Golgi apparatus appears normal. However, there are significant distinctions in the behavior of cell lines derived from different tissue origin. Whereas B16 cells of fibroblast-like origin and parenchymal BRL cells easily adopt a 3D morphology, A549 epithelial cells do either not invade the 3D patterns or remain associated with the lateral surfaces of the wheels. Analyzing the cell volume ($\mu m^3$) of several cell lines we observed that fibroblast-like cells (MEF, BRL, B16) have a larger cell volume in the 3D scaffolds while the cell volume for epithelial-derived cells (NRK, A549) does not vary depending on the substrate dimensionality (Fig. 9). These findings indicate, that the ability to adopt a 3D growth morphology is cell type depended, but that the intracellular morphology and the molecular composition of cell contact sites of fibroblast-like cells is not considerably altered when they grow in a stiff 3D environment.

stmeyer

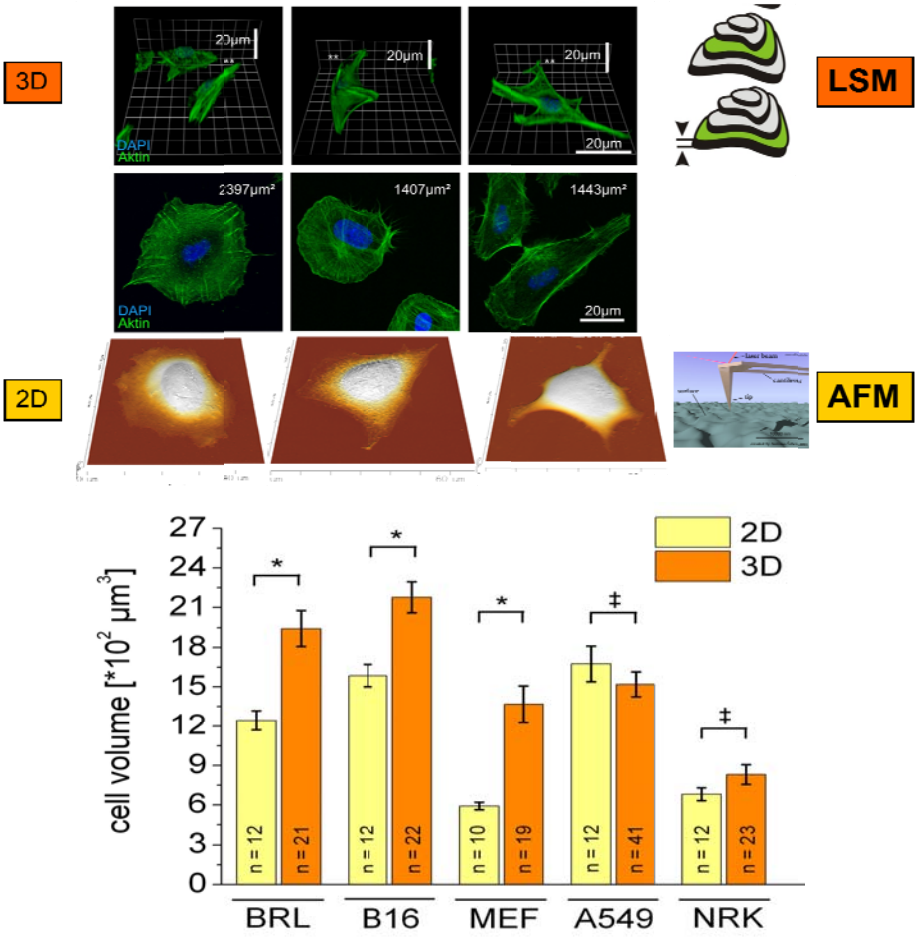


**Figure 9** Cell volume differs between 2D and 3D cell culture. Five different cell lines were grown on 2D glass substrates or in 3D scaffolds. Cell volume was measured with an AFM (collaboration with Clemens Franz, E2.4) for 2D cultures and calculated from LSM image stacks for 3D cultures. Fibroblast-like cells (MEF, BRL, B16) have a larger cell volume in the 3D scaffolds while the cell volume for epithelial-derived cells (NRK, A549) does not vary depending on substrate dimensionality.

Apart from the three-dimensionality of the growth substrate, the stiffness of the surrounding scaffold has also been shown to influence cell fate. Mechanically flexible 3D structures were realized using different photoresits. Ormocer® proved to be a useful material to produce rugged but elastic 3D templates that can be deformed by forces applied by single cells (Klein et al., 2010). Primary cardiomyocytes from chick embryos were cultured in 3D Ormocer® templates. After 1-2 days these cells spontaneously start to rhythmically contract and were imaged with video microscopy. After fixation the cells were immunostained and analyzed with a confocal microscope. Figure 10 depicts an example of a cardiomyocyte growing in a 3D structure consisting of pillars of 10 µm in height connected by beams of 1 µm in diameter. Still frames of video images demonstrate that a cross brace in contact with the cell is deformed by 1 µm during a single contraction cycle and then released into its original position. (Fig. 10 c,d). In collaboration with Clemens Franz (E2.4), the mechanical properties of similar structures were determined using an AFM. These calibrations show that a deformation of the cross braces by 1 µm corresponds to a force of 50 nN.

Our results demonstrate for the first time that is feasible to produce rugged but elastic 3D templates that can be deformed by single heart muscle cells (Klein et al., 2010).

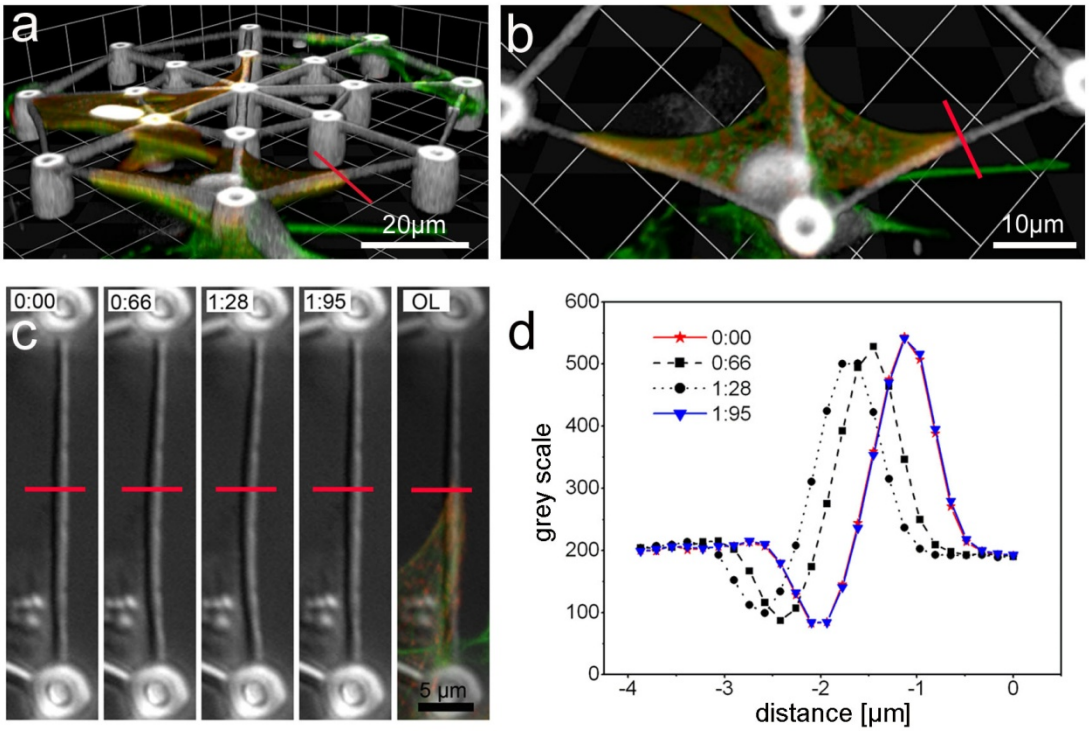


**Figure 10**. Primary cardiomyocytes were cultured in flexible 3D-Ormocer® templates and imaged with video microscopy. After fixation cultures were immunostained for actin (green), α-actinin (red), and DNA (white) and analyzed with a confocal microscope (**a**) 3D reconstruction of a template consisting of pillars connected with thin cross braces. (**b**) Top view of confocal image stack depicting the cardiomyocyte growing in front of the template (**c**) Still frames of the video images showing the cross brace marked with a red line in (b). During rhythmic contractions of the cadiomyocyte the cross brace is deformed by the cell. Time is given in minutes and seconds. (**d**) Graph showing grey scale levels along the red line for the time points depicted in (c). During a single beating cycle, the cross brace is pulled inwards by the cell for about 1 µm and then released into its original position.

The DLW scaffolds described so far have been homogeneously coated with ECM molecules. Ideally, 3D scaffolds should rather have an adjustable distribution of cell-substrate contact sites to manipulate cell adhesion and cell shape in all three dimensions. Tailored 3D scaffolds with a controlled ECM distribution were realized by sequential DLW of two different photoresists (Klein et al., 2011). Composite-polymer scaffolds with distinct protein-binding properties were fabricated and selectively bio-functionalized thereafter (Fig. 11). For small protein-binding cubes in the scaffolds we selected Ormocomp®, a member of the inorganic (Si-O-Si)–organic hybrid polymer Ormocer® family. For the protein-repelling frameworks we choose a photoresist composed of the monomer polyethylene glycol diacrylate (PEG-DA). Polyethylene glycol-based surface modification is widely used for conventional 2D patterns to prevent unspecific protein adsorption and cell attachment. Physical scaffold stability was be achieved by combining PEG-DA with the polyacrylate crosslinking agent pentaerythritol tetraacrylate (PETA).

When these composite 3D scaffolds were incubated with a fibronectin (FN) solution, the ECM protein binds preferentially to the Ormocomp® cubes as detected by immunofluorescence labeling (Fig. 12). Dissociated chicken fibroblasts were cultured in these scaffolds for two hours, fixed, immunostained for actin and Paxillin, and analyzed by confocal microscopy. Within the 3D scaffold, cells either adhered to a single Ormocomp® cube or spread and formed connections to several cubes (Fig. 12). In doing so, cells often connect cubes on beams in different heights, revealing a true 3D growth pattern. Here, concave arc-like actin fibres line the cell periphery between the adhesion points as described for geometrically similar 2D patterns (see above). At present we are investigating, in collaboration with the group of Ulrich Schwarz, whether the same rules and theoretical models developed for 2D cell culture also apply for cell forms in 3D scaffolds.

To summarize, we show that cell adhesion and consequently cell shape can be fully controlled in 3D for the first time. This method opens new possibilities to systematically study the effects of spatial ligand distributions and mechanical scaffold stiffness on cell behavior in 3D environments.

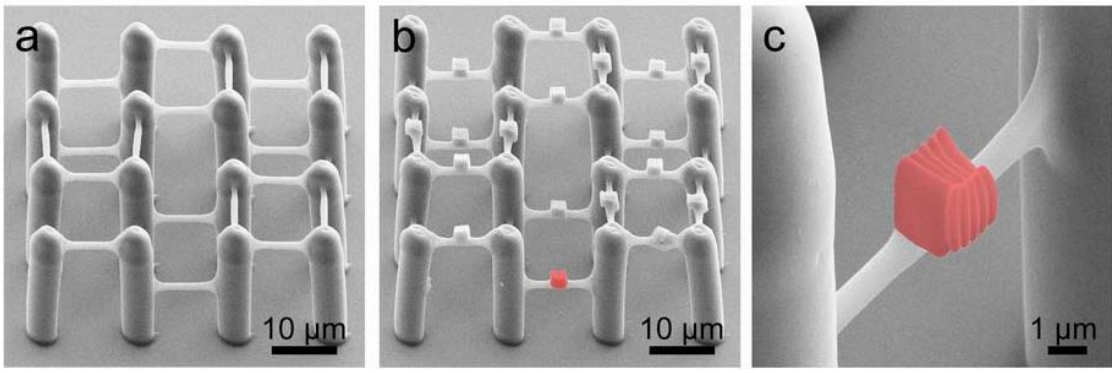


**Figure 11**. Scanning electron micrographs illustrating the fabrication of 3D composite-polymer scaffolds by sequential Direct Laser Writing (DLW). **(a)** In a first step, 3D frameworks consisting of protein-repellent poly(ethylene glycol) diacrylate (PEG-DA) with 4.8% pentaerythritol tetraacrylate (PETA) are polymerized and developed. **(b)** Frameworks are then casted with the photoresist Ormocomp® and cubes (one cube is highlighted in red) are precisely positioned to the PEG-DA beams in a second DLW step. **(c)** Higher magnification image of an Ormocomp® cube (highlighted in red).

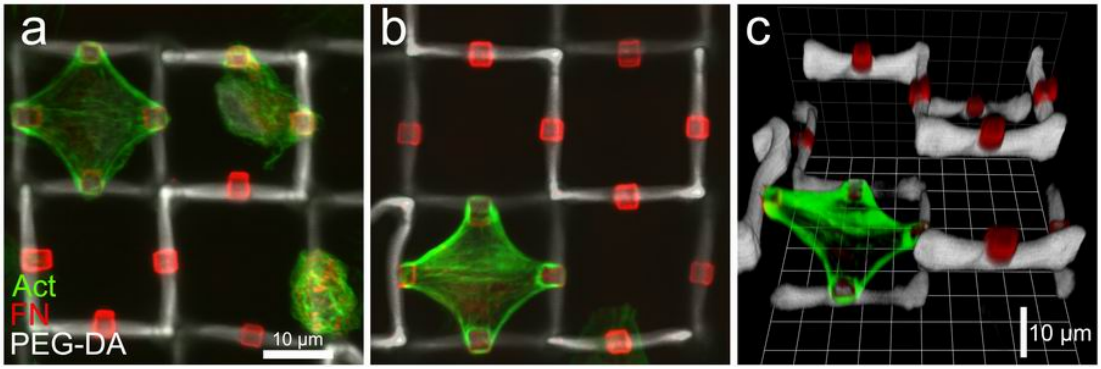


**Figure 12**. Cell growth in 3D composite-polymer scaffolds. Primary chicken fibroblasts are cultivated in the scaffolds and immunostained for fibronectin (FN) (red) and f-actin (green) and Paxillin. **(a)** Top view of a confocal image stack depicting cells adhering to one, two, or three FN-positive Ormocomp® cubes. **(b)** Top view and **(c)** 3D reconstruction of a confocal image stack depicting a single cell adhering to Ormocomp® cubes in different heights.

Another advantage of using PEG-DA for the protein-repelling frameworks is the fact that the elastic properties can be tuned by using varying amounts (1-10%) of PETA (Klein et al., 2011). These functionalized and elastic 3D scaffolds are currently employed to measure forces applied by single fibroblasts to their 3D environment with respect to adhesion geometry (Fig. 13).

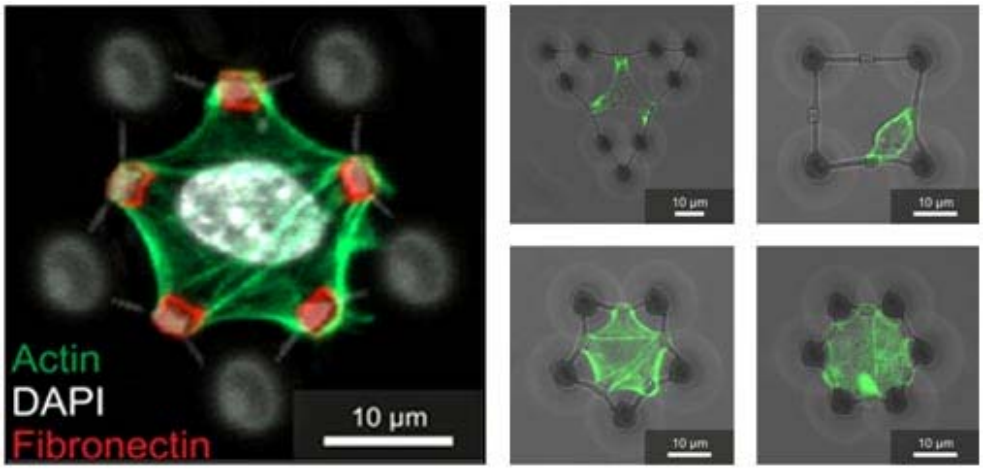


**Figure 13**. Cell growth in flexible 3D composite-polymer scaffolds. Forces of single cells exerted to elastic beams attached to stiff pillars are investigated with respect to the substrate geometry.

The *long term perspective* of this project will be to realize flexible 3D templates with a multiple bio-functionalization, e.g. adhesive RGD-peptides or ECM-proteins in combination with signaling molecules like cadherins or ephrins (Delaittre et al., 2012). Applicable flexible polymers will be developed by the group of Barner-Kowollik (E2.6). This collaboration has already been started in June 2010 with Dr. Delaittre (Humboldt Fellow) and a PhD student (VCI Fellow). Photoactive clickable substrates will be incorporated in the polymer compounds and selectively activated after DLW by UV-light. First approaches in this direction were recently published (Pauloehrl et al., 2011). These processes require the use of different wavelengths for the DLW and the polymer activation step. A corresponding DLW setup equipped with a tunable laser and the expertise will be available via collaboration with subproject A1.4. Suitable biomolecules (e.g. SNAP or CLIP-tagged cadherins, tagged RGD-peptides) for functionalization will be obtained from the groups of D. Wedlich (E2.2) and L. Fruk (E1.6). The development of these methods will open new possibilities to systematically study the effects of spatial ligand distributions and mechanical scaffold stiffness on cell behavior in 3D environments.

**Literature**

T. Autenrieth and M. Bastmeyer. Micropatterned fibronectin-gradients induce polarization and haptotaxis in primary fibroblasts. Eur. J. Cell Biol. 89: 19 (2010)

I.B. Bischofs, F. Klein, D. Lehnert, M. Bastmeyer, and U.S. Schwarz, Filamentous Network Mechanics and Active Contractility Determine Cell and Tissue Shape, Biophys. J. 95: 3488 (2008).

G. Delaittre, A.M. Greiner, T. Pauloehrl, M. Bastmeyer and C. Barner-Kowollik. Chemical approaches to synthetic polymer surface biofunctionalization for targeted cell adhesion. Soft Matter: invited review (2012, in press).

F. Klein, T. Striebel, J. Fischer, Z. Jiang, C.M. Franz, G. von Freyman, M. Wegener and M. Bastmeyer. Elastic fully three-dimensional microstructure scaffolds for cell force measurements. Adv. Mater. 22, 868 (2010)

F. Klein, B. Richter, T. Striebel, C.M. Franz, G. von Freyman, M. Wegener and M. Bastmeyer. Two-Component Polymer Scaffolds for Controlled Three-Dimensional Cell Culture. Adv. Mater. 23: 1341 (2011)

A.M. Greiner, B. Richter and M. Bastmeyer. Tailored micro- and nanoengineered 3D scaffolds for cell culture studies. Macromol. Biosci.: invited Feature Article (2011, in press)

S. Lang, A.C. von Philipsborn, A. Bernard, F. Bonhoeffer, and M. Bastmeyer, Axon Guidance in Ephrin Gradients Produced by Microfluidic Networks, Anal. Bioanal. Chem. 390, 809 (2008)

D. Lehnert, B. Wehrle-Haller, C. David, U. Weiland, C. Ballestrem, B.A. Imhof, and M. Bastmeyer,Cell Behaviour on Micropatterned Substrates: Limits of Extracellular Matrix Geometry for Spreading and Adhesion, J. Cell Sci. 117: 41 (2004)

T. Pauloehrl, G. Delaittre, M. Bastmeyer and C. Barner-Kowollik. Ambient Temperature Polymer Modification by In-situ Phototriggered Deprotection and Thiol-Ene Chemistry. Polym. Chem.: DOI: 10.1039/c1py00372k (2011).

A.C. von Philipsborn, S. Lang, A. Bernard, J. Loeschinger, C. David, D. Lehnert, M. Bastmeyer, and F. Bonhoeffer, Microcontact Printing for Generation of Graded Patterns of Axon Guidance Molecules Nature Protocols: DOI: 10.1038/nprot.2006.251 (2006a)

A.C. von Philipsborn, S. Lang, J. Loeschinger, A. Bernard, C. David, D. Lehnert, F. Bonhoeffer, and M. Bastmeyer, Growth Cone Navigation in Substrate-Bound Ephrin Gradients, Development 133, 2487-2495 (2006b)

A.C. von Philipsborn and M. Bastmeyer, Mechanisms of Gradient Detection: A Comparison of Axon Pathfinding with Eukaryotic Cell Migration, Int. Rev. Cytol. 263, 1 (2007a)

A.C.von Philipsborn, S. Lang, Z. Jiang , F. Bonhoeffer, and M. Bastmeyer, Substrate-Bound Protein Gradients for Cell Culture Fabricated by Microfluidic Networks and Microcontact Printing, Science STKE: DOI: 10.1126/stke. 4142007pl62007 (2007b)

A.F. Ross, Z. Jiang, M. Bastmeyer and J. Lahann. Physical Aspects of Cell Culture Substrates: Topography, Roughness, and Elasticity. Small (2011, in press)